Biodegradable thermomagnetically responsive soft untethered grippers

Kunihiko Kobayashi[#†§], ChangKyu Yoon[#‡†], Seung Hyun Oh[†], Jayson V. Pagaduan[†] & David H. Gracias[*‡†]

[†]Department of Chemical and Biomolecular Engineering, The Johns Hopkins University, Baltimore, MD 21218, USA.

[‡]Department of Materials Science and Engineering, The Johns Hopkins University, Baltimore, MD 21218, USA.

[†]Present address: Department of Mechanical Systems Engineering, Sookmyung Women's University, Seoul, Republic of Korea.

[§]JSR Corporation, 1-9-2, Higashi-Shimbashi, Minato-ku, Tokyo 105-8640, Japan.

[#] K. Kobayashi and Dr. C. Yoon contributed equally to this work.

* Corresponding Author: email: dgracias@jhu.edu

KEYWORDS: *stimuli responsive materials, hydrogels, soft robotics, bioMEMS, actuators*

ABSTRACT

Soft-robotic devices such as polymeric microgrippers offer the possibility for pick-and-place of fragile biological cargo in hard to reach conduits with potential applications in drug delivery, minimally invasive surgery and biomedical engineering. Previously, millimeter-sized self-folding thermomagnetically responsive soft-grippers have been designed, fabricated, and utilized for pick-and-place applications but there is the concern that such devices could get lost or left behind after their utilization in practical clinical applications in the human body. Consequently, strategies need to be developed to ensure that these soft-robotic devices are biodegradable so that they would disintegrate if left behind in the body. In this paper, we describe the photopatterning of bilayer gels composed of a thermally responsive high swelling poly[oligo ethylene glycol methyl ether methacrylate (M_n=500)-bis(2-methacryloyl)oxyethyl disulfide], P(OEGMA-DSDMA) and a low swelling poly[acrylamide- *N*, *N*'-bis(acyloyl) cystamine], P(AAm-BAC) hydrogel in the shape of untethered grippers. These grippers can change shape in response to thermal cues and open and close due to the temperature induced swelling of the P(OEGMA-DSDMA) layer. We demonstrate that the grippers can be doped with magnetic nanoparticles so that they can be moved using magnetic fields or loaded with chemicals for potential applications as drug-eluting theragrippers. Importantly, they are also biodegradable at physiological body temperature (~ 37 °C) based on cleavage of disulfide bonds by reduction. This approach which combines thermoresponsive shape change, magnetic guidance, and biodegradability represents a significant advance to the safe implementation of untethered shape change biomedical devices and soft-robots for medical and surgical applications.

INTRODUCTION

Untethered micro- and milli-robots offer the possibility for less invasive and smart medical interventions.[1–3] In contrast to robots that are controlled by wires and tethers, untethered robots can be miniaturized, deployed in large numbers, operated in parallel, and manipulated in hard to reach and tortuous conduits. Typically, these devices utilize changes in material properties in response to an external or local stimulus to drive actuation. A popular strategy is to utilize differentially responsive swelling in bilayer hydrogels to drive shape change and consequently gripping, transport, excision and drug-eluting functionalities of broad relevance to medicine.[4–9] These bilayer devices typically consist of a high swellable gel layer which expands or contracts significantly in aqueous media in response to a specific stimulus and a low swellable gel or polymer which does not expand or contract appreciably. As previously demonstrated, many stimuli that are compatible with clinical interventions such as temperature, pH, light and even DNA, can be used to swell or contract the active gel to open or close the devices, offering the possibility for triggered or autonomous responses in-vivo.[10–12]

We have previously described self-folding thermomagnetically responsive soft-microgrippers and have utilized these extensively both in-vitro and in-vivo using either manual or robotic platforms.[13,14] The devices have been utilized to grip tissue, deliver drugs, biopsy cells or pick-and-place soft cargo. However, as with these and other untethered soft-robotic devices, a significant concern in utilization in-vivo is that even with state-of-the-art imaging guidance and manipulation, they could get stuck or left behind in the body. In specific locations such as on the gastrointestinal (GI) mucosa which self-renews and clears every few days, small devices would be expelled from the body and pose minimal risk.[15] However, for larger devices and utilization in other areas of the body other than the GI tract, retention represents a serious concern. For example, retention risks have been observed in capsule endoscopy, and although the risks are small, they sometimes require endoscopic or quite invasive surgical intervention to resolve.[16] The retention risks would increase especially if the device has sharp edges as in the case of gripping devices.

An attractive strategy to reduce the risks associated with retention is to create shape changing devices that are endowed with the biodegradability of conventional drug delivery systems.[17,18] However, incorporating this feature is a challenge since many stimuli responsive materials such as N-isopropylacrylamide (NIPAM) are not naturally biodegradable; and synthetic modifications are needed to endow hydrogels with both stimuli responsivity and biodegradability.[19,20] Among the effective strategies to endow biodegradability is the incorporation of disulfide bonds that can be readily cleaved by reduction.[21,22] Disulfide bonds are present in many proteins and drugs, and are broken by thiols such as glutathione (GSH), which is present in millimolar concentrations within the cells and micromolar concentrations outside the cells.[21] In contrast to alternate strategies to endow biodegradability such as the synthesis of gels with ester bonds that are cleaved by acid or base so as to degrade in the low pH of the stomach, degradability of disulfide-containing hydrogels can be controlled using biocompatible reducing agents such as cysteine, GSH or even ascorbic acid (Vitamin C).

Consequently in our approach we utilized hydrogels linked by disulfide bonds and composed of a high swellable poly(oligo ethylene glycol methyl ether methacrylate- bis (2-methacryloyl) oxyethyl disulfide) (M_n=500), [POEGMA-DSDMA)] with a relatively non swellable poly(acrylamide-*N*, *N*'- bis (acryloyl) cystamine), [P(AAm-BAC), passive gel]. We developed a photopatterning process that allowed us to construct different gel patterns with precision, and in a parallel manner. These gels could be structured in arbitrary shapes including overlay with spatial registry to form hand shaped grippers. Biocompatible iron-oxide nanoparticles and chemicals could be incorporated in the gels during processing so that magnetic fields could guide the grippers and release chemicals. Based on the combined attributes of the grippers, we highlight thermally responsive actuation, pick-and-place of fragile cargo, drug elution and biodegradability at physiological temperatures.

MATERIALS AND METHODS

Materials

Acrylamide (AAm, Sigma-Aldrich), Oligoethylene glycol methyl ether methacrylate M_n=500 (OEGMA, Sigma-Aldrich), *N*,*N*'-bis(acryloyl)cystamine (BAC, Alfa Aesar), Bis(2-methacryloyl)oxyethyl disulfide (Disulfide based dimethacrylate or DSDMA, Sigma-Aldrich), dimethyl sulfoxide (DMSO, Fisher Scientific), sodium alginate (Na-Alginate, Sigma-Aldrich), Irgacure 2100 (Ciba), acetone (Fisher Scientific), methanol (Fisher Scientific), isopropyl alcohol (IPA, Fisher Scientific), Fe_2O_3 NPs (Sigma-Aldrich product #544844, <50 nm particle size), CYTOP® (CTL-809M, AGC Asahi glass), SC 1827 (Microposit) and GSH (Sigma-Aldrich) were used as received.

Preparation of photopatternable OEGMA-DSDMA and AAm-BAC pre-gel solutions

An OEGMA-DSDMA stock solution was prepared by mixing OEGMA and DSDMA in a ratio of 95.2:4.8 (wt:wt). Then, the photoinitiator Irgacure 2100 (Ciba) was added to the OEGMA-DSDMA solution in a ratio of 1:100 (v/v). The solution was mixed thoroughly by vortexing overnight using a magnetic stir bar. The AAm-BAC stock solution was prepared by mixing AAm and BAC with in a ratio of 70:30 (wt:wt) and it was dissolved in DMSO at a concentration of 20%. Then, the solution was vortexed overnight using a magnetic stir bar. This stock solution was then mixed with Irgacure 2100 in a ratio of 100:1 (v/v) just before UV light exposure. To visualize the photolithographically defined patterns (Figures 2B and 2C), rhodamine 6G was added to the pre-gel solutions.

Photopatterning of P(OEGMA-DSDMA) and *P(AAm-BAC) bilayer hydrogels*

The P(AAm-BAC) and P(OEGMA-DSDMA) gels were patterned using multilayer, contact-mode photolithography. First, 150 µl of the AAm-BAC passive gel solution was injected between a Na-alginate coated glass slide and CYTOP® coated Cr mask with approximately a 32 µm thick spacer. Then, a UV spot curing lamp with an intensity of 36 mJ/cm^2 was used to polymerize the AAm-BAC solution for

approximately 20 seconds. After photopatterning, the chambers were taken apart and the cross-linked patterns on glass slide part were rinsed several times with IPA and then dried using N_2 gas. The relatively high swelling gel layer was patterned on top of the low swelling gel layer to form a bilayer as follows. First, 300 μl of OEGMA- DSDMA solution was injected into the chambers with one more 32 μm thick spacers. After precisely aligning the pattern with the previously patterned P(AAm-BAC) layer, the OEGMA- DSDMA solution was photopatterned using a UV lamp with an intensity of 36 mJ/cm^2 for approximately 20 seconds. After photopatterning, the chambers were taken apart, and the glass slide was washed gently with isopropanol (IPA) and then dried with nitrogen (N_2) gas. Finally, the P(AAm-BAC) and P(OEGMA-DSDMA) bilayer patterns were lifted off from the glass slide by dissolving the Na-alginate sacrificial layer in 1x PBS buffer solution. After the photopatterned gels were released from the glass substrate, they were stored at room temperature until they reached a fully swollen equilibrium state. See supplementary information for additional details on the choice of concentration for each gel.

Synthesis of magnetically responsive and fluorescent soft grippers

To synthesize magnetically responsive soft grippers, 1 wt % biocompatible magnetic iron oxide (Fe_2O_3) nanoparticles (NPs) were mixed with the AAm-BAC solution before UV light exposure. Grippers for dye/chemical release experiments were prepared by immersing the grippers in a solution of rhodamine 6G dissolved in 1x PBS buffer at a concentration of 10 mg/ml overnight. Fluorescent grippers (Figure 4C) were synthesized by mixing 0.1 % methacryloxyethyl thiocarbamoyl rhodamine B fluorescent monomer with the pre-gel solution before UV exposure.

Characterization of actuation, biodegradability, and dye diffusion properties of the soft grippers

The actuation of the soft grippers was characterized by heating in an aqueous environment in a Petri dish or cooling by air and was visualized using an optical microscope (AZ 100, NIKON). The profile of actuation was quantified by measuring and plotting the average of the normalized tip-to-tip distance at different temperatures divided by the patterned tip-to-tip distance (L/L_0) of the grippers at each

temperature. The image analysis was done using the Image J software. Grippers were manipulated using a permanent bar magnet that was maneuvered over the Petri dish and fragile biological cargo used for pick-and-place experiments was soft tofu (House foods "Premium Tofu - Soft").

The biodegradation studies using GSH were performed in 100 mM phosphate buffer pH=7.4 containing 100 mM NaCl and variable concentrations of GSH between 0.05 to 50 mM at 37 °C. The biodegradation study using ascorbic acid was performed in 500mM ascorbic acid and 500 mM hydrogen peroxide at 37 °C.

For dye release experiments, the magnetic rhodamine 6G loaded grippers were first rinsed in 1x PBS buffer and then transferred into a fresh buffer solution. The dye release was visualized using fluorescence microscopy.

Cell viability assay

Immortalized human aortic endothelial cells (hTERT HAEC) were grown in 24-well plates in endothelial cell growth media at 37 °C and 5% CO_2. Cells were seeded at a density of 1.95 x 10^5 cells/well. After 24 hours of seeding, wells were replenished with fresh culture media. Cells were cultured for three more days without grippers (control sample), with either the grippers or the GSH solution alone, and with the combined gripper and GSH solution. An MTT assay was performed after three days. Formazan crystals were dissolved in dimethyl sulfoxide and the absorbances were measured at 570 nm and 650 nm using a SpectraMax i3 multi-well plate reader. Viability measurements were normalized using the reading from the control sample.

RESULTS AND DISCUSSION

The conceptual illustration of the soft biodegradable grippers is shown in **Figure 1**. The grippers are composed of bigel patterns of a thermally responsive photocrosslinked relatively high swelling P(OEGMA-DSDMA) gel and a low swelling P(AAm-BAC) gel doped with Fe_2O_3 nanoparticles (**Figure**

1A). POEGMA is a well-known thermally responsive hydrogel with tunable thermal response between 20 to 90 °C based on a low critical solution temperature (LCST) in aqueous media; the LCST can be tuned by varying the side chain length.[23–26] The OEGMA prepolymer is conjugated with DSDMA; the latter endows biodegradability based on the reduction of disulfide bonds. The photocrosslinking is done using free radical polymerization of the acrylate groups on OEGMA and DSDMA, initiated by the UV excitation of the photoinitiator Irgacure **(Figure S1)**. The low swelling P(AAm-BAC) gel is also photocrosslinked using free radical polymerization of AAm and BAC monomers. This gel does not swell appreciably because of lack of pendant groups and specific formulation (discussed later). Like the P(OEGMA-DSDMA) gel, the P(AAm-BAC) gel also contains disulfide bonds; hence, both gels biodegrade in the presence of intercellular, intracellular or added disulfide reducing agents (**Figure 1B**, **Figure S2**). Importantly, the degradation byproducts are uncrosslinked polymers as opposed to monomers which are generally considered more toxic. For example, acrylamide is generally considered toxic while polyacrylamide is less problematic and widely utilized in a number of products including in cell culture.[27,28]

Since both gels can be photopatterned, we can utilize CAD designed photomasks to pattern arbitrary shapes. However, since the gels are soft and sticky, additional steps are needed to photopattern the gels. Specifically, in order to obtain a high lateral resolution of hydrogel patterns while resolving adhesion or edge effect problems during fabrication, we primarily considered contact-mode chambers.[29] Each chamber is composed of a hydrophobic CYTOP® coated chromium (Cr) mask[12] and sodium alginate (Na-Alginate) sacrificial layer coated glass substrate with two 32 μm thickness spacers (**Figure 2A**). We tested a variety of geometric parameters of shapes, sizes, and thickness of monolayer hydrogels according to different UV light exposure dosages. Regarding shape, we designed long bar, triangle, square, round, and star shapes to validate the robust, high yield and mass producible photopatterning of both P(OEGM-DSDMA) and P(AAm-BAC) gels (**Figure 2B**, **2C**). Since the gels are optically transparent and hard to visualize, a highly fluorescent rhodamine 6G dye could be added to the pre-gel gel,

before photopatterning for visualization. Based on our studies, we estimate that the photopatterning process could resolve features as small as 50 μm.

After developing the photopatterning process for each gel separately, we photopatterned them on top of each other using two photopatterning steps with registry between photomasks of the two layers to form a composite hand shaped gripper (**Figure S3**). The grippers are composed of a continuous high swelling P(OEGMA-DSDMA) layer on top of discrete low swelling P(AAm-BAC) gel patterns (see Materials and Methods for details). The photopatterned bigel grippers could be released from the glass slides by dissolving the Na-Alginate sacrificial layer in DI water or 1xPBS. After release, the grippers were stored in a vial for 10 hours, where the high swelling layer equilibrated to its fully swollen state. In this state, the grippers were folded shut (**Figure 2D** and **Video S1**) and opened up on heating. In order to investigate the thermally responsive actuation, we took videos and obtained snapshots of the grippers at different stages of the folding and unfolding process. We measured the end tip-to-tip length ratio (L/L_0) of the grippers at different temperatures between 30 °C and 72 °C. Here, L represents the tip-to-tip distance at each temperature and L_0 is the tip-to-tip distance as patterned. A larger L/L_0 indicates that the gripper is open while a smaller one indicates that the gripper is closed.

We observed a transition in the temperature range between 50 and 70 °C (**Figure 2E**) with closing at the lower temperatures and opening at the higher temperatures. We note that the difference in heating and cooling response can be attributed to differences in the heating and cooling rates which were different. The inset in **Figure 2E** shows the temperature ramp during heating and cooling cycles. We heated the Petri dish on a hot plate while cooling was achieved by turning off the hot plate and using the ambient air to cool. In general, the heating rate was higher than the cooling rate.

We attribute the unfolding or opening of the gripper to deswelling or shrinking of the P(OEGMA-DSDMA) gel which becomes hydrophobic above its volume transition temperature and folding or closing of the gripper to the swelling of the P(OEGMA-DSDMA) gel which becomes hydrophilic below its

volume transition. During the process, we observed that the dimensions of the low swelling P(AAm-BAC) segments remain relatively unchanged and are on the inside of the folded or closed gripper. This opening and closing between 50 °C and 70 °C and were verified by 30 cycles with no visible delamination between layers. This actuation mechanism of the P(OEGMA-DSDMA)/P(AAm-BAC) soft grippers also agrees well with our previous thermal response actuation studies and simulations of poly (N-isopropylacrylamide-co-acrylic acid) (pNIPAM-AAc) and polypropylene fumarate (PPF) as well as POEGMA bilayers.[13,30]

We investigated the effect of the concentration of DSDMA or BAC on the linear swelling ratio (**Figure S4A**) and patterned shape of the gripper (**Figure S4B**). It should be noted that both molecules have two polymerizable functionalities (vinyl groups) in their structure, and consequently they act as crosslinkers during polymerization and a variation in their concentration can have a dramatic effect on the properties of the cross-linked gel. To measure the swelling ratio, we photopatterned 1.7 cm x 1.7 cm square gel shapes with different crosslinker ratios and equilibrated in 1xPBS at room temperature for overnight. We measured the equilibrated length and evaluated the linear swelling ratio and plotted this as a function of the monomer concentration (**Figure S4A**). We observe that with an increase in the concentration of BAC in the P(AAm-BAC) gel, the swelling ratio decreased as expected and the patterned shape of the gripper changed from open to loosely closed to very tightly closed. We rationalize this observation by noting that an increase in the concentration of BAC results in a more highly crosslinked or less swellable gel. Likewise, an increase in the DSDMA concentration also resulted in lower swelling; consequently, based on the concentration the swelling ratio could be tuned. Based on these experiments we determined an optimal crosslinker composition for the P(OEGMA-DSDMA)/P(AAm-BAC) bilayer grippers of 4.8% DSDMA in P(OEGMA-DSDMA) to create a high swelling gel and 30% BAC in the P(AAm-BAC) to create a low swelling gel. The maximum volumetric swelling ratio for high swelling P(OEGMA-DSDMA) and low swelling P(AAm-BAC) is approximately 463% and 58% respectively.

A popular strategy to enable remote manipulation of soft robots is to endow them with magnetic responsivity.[13,31–35] We mixed iron oxide nanoparticles (Fe_2O_3 NPs) inside the passive P(AAm-BAC) gel layer. We observed that gels with Fe_2O_3 NPs required a higher UV irradiation intensity for cross-linking compared to gels without the NPs, arguably. When an optimized concentration of approximately 5.3% (w/w) Fe_2O_3 was incorporated with P(AAm-BAC) hydrogel, we observed no significant effects on the thermoresponsive actuation of the grippers (**Figure 3A, 3B**) and grippers closed reliably as evidenced by snapshots of multiple open and closed grippers. Due to the magnetic feature of the grippers, it was possible to achieve the important robotic task of pick-and-place which is ubiquitous in macroscale robotics such as the assembly line as well as of critical importance in medicine; for instance, in the placement of stents or delivery of embolization devices. Sequential optical images highlight the pick-and-place of a piece of soft-cargo (soft-tofu, a gel with an estimated modulus in the range of 1-5 KPa)[36] using P(OEGMA-DSDMA)/ Fe_2O_3 embedded P(AAm-BAC) grippers (**Figure 3C**). We note that the modulus of this cargo is similar to that of many endothelial, and stromal tissues.[37]

Briefly, the gripper was heated and guided to soft-cargo target using a permanent bar magnet with visual guidance. On cooling below the transition temperature, the gripper closed its fingers and grabbed the target. The gripper with the cargo in its grasp was then guided to another site and warmed above the transition temperature to release the cargo (**Video S2**). Consequently, it was possible to pick-and-place the soft cargo without any visible damage, as verified by optical microscopy (**Figure 3C**). This experiment highlights the use of soft gel based robotic appendages for manipulation of fragile cargo.

In addition to pick-and-place, another possible use for such devices is in drug delivery. Self-folding devices have previously been utilized to latch onto tissues and release drugs.[8,38] Like in previous descriptions of so called theragrippers,[8] multi-finger actuators can potentially grip onto tissue and function as a sustained release patch on the inside of the body. Similar to theragrippers, we showed that our magnetically guidable grippers could also be potentially loaded with drugs for thermally actuatable

drug patch applications. We incorporated rhodamine 6G dye into the grippers and visualized release of the dye by diffusion in 1x PBS buffer, pH=7.4 buffer at 25 °C (**Figure 3D and Video S3**).

A major advance reported in this paper is the creation of simultaneously biocompatible and biodegradable multifunctional soft-robotic functional structures. We verified the cellular biocompatibility of these hydrogel grippers for three days of contact periods using hTERT HAEC cells with 1.95 x 10^5 /well to ensure that there were no cytotoxic components. We used a standardized test for in-vitro evaluation of cytotoxicity of medical devices; ISO 10993-5.[39] In all our samples, which consisted of grippers, grippers with GSH, and a GSH control we observed over 70 % cell viability, (%= OD_{570} / $OD_{570,\ blank}$ x 100) (**Figure 4A**) which indicates a non-cytotoxic index based on this ISO standard.[40]

We investigated the biodegradability of our untethered grippers at the physiological body temperature in the presence of reducing agents as per the mechanism shown in **Figure S2**. We analyzed biodegradability, visually by measuring the disappearance of the gels. Using optical microscopy, we measured the degradation time of the P(OEGMA-DSDMA) gel layer in the bilayer grippers in 100mM phosphate buffer containing 100mM NaCl and GSH, with GSH concentration in the range of 0.05mM-50mM (**Figure 4B**). Our results indicate that degradation is controllable as a function of GSH concentration and as can be sped up by adding GSH.

Previously, we have noted that intracellular GSH concentrations are in the millimolar range and extracellular concentrations are in the micromolar range, so degradation of robotic micro and nanostructures composed of these gels could potentially occur in native environments.[41] In addition, GSH can also be administered via oral (up to 3 g/day), intravenous (up to 2.4 g/day), intramuscular (up to 0.6 g/day), and aerosol (up to 1.2 g/day) routes with no severe side effects.[42] Hence, the time scale of biodegradation can be varied and tuned.

In addition to the concentration of GSH, we investigated the influence of the composition and UV exposure time during patterning of the P(OEGMA-DSDMA) gels on their biodegradation in 100 mM

phosphate buffer containing 50mM GSH and 100mM NaCl for 24H. Cubic P(OEGMA-DSDMA) gels were fabricated with different pre-gel solutions and different UV exposure times. The pre-gel solutions consisted of OEGMA, DSDMA and DMSO. OEGMA and DSDMA which are the reactive components and DMSO functions as a solvent and not a reactive component. The weight ratio of DSDMA and OEGMA was fixed at DSDMA:OEGMA=4.8: 95.2 in all the pre-gel solutions while the weight ratio of DSDMA, OEGMA and DMSO were varied in three levels, (DSDMA+OEGMA):DMSO=100:0, 80:20 and 60:40 (Column 2 in Table S1) and exposed to UV light for different times (Column 3 in **Table S1**). We observed that the P(OEGMA-DSDMA) gels that were crosslinked at short UV exposure times or at a concentration of (DSDMA+OEGMA):DMSO=60:40 degraded entirely in the GSH solution at physiological body temperature (37 °C). The gels fabricated at other conditions just swelled (expanded) in the GSH solution but did not degrade (Column 3 in **Table S1**). We attribute this observation of enhanced biodegradation to a lower extent of crosslinking in the gel which had a lower monomer concentration and was photocrosslinked at shorter UV exposure times.

Independently, we prepared cube shaped P(AAm-BAC) gels and performed biodegradation test in 100 mM phosphate buffer containing 50mM GSH and 100mM NaCl for 24H. Cubic P(AAm-BAC) gels were fabricated from pre-gel solutions composed of AAm, BAC, and DMSO and the optimal concentration ratio of AAm:BAC in the solution was 97.3:2.7 and AAm+BAC:DMSO was 20:80 for complete biodegradation (**Figure S5A**).

Using optimal conditions for swelling and biodegradation, we then designed and fabricated functional bilayer grippers which fully degrade in GSH. For example, as shown in **Figure 4C**, the P(OEGMA-DSDMA) gel layer of the bilayer grippers completely degrades in four hours, and the P(AAm-BAC) gel layer of the bilayer grippers degrades more slowly and disappears in 20 days in 100 mM phosphate buffer containing 100 mM NaCl and 50 mM GSH at 37 °C. Notably, as soft gripping devices, we observed that the grippers lose their ability to grip objects with full degradation of

P(OEGMA-DSDMA) layer. We observed that the grippers broke into small pieces when the P(OEGMA-DSDMA) gel layer of the bilayer grippers wholly degraded.

In addition to GSH, we also explored the biodegradability of the soft grippers in a medium containing 500 mM ascorbic acid and 500 mM hydro peroxide at pH 3 (**Figure 4D, Figure S6**). Ascorbic acid, well known as a water-soluble form of Vitamin C, an essential vitamin, can also function as a disulfide reducing agent.[43] Thus, it can be utilized as an alternate reducing agent for our biodegradable soft grippers. As described in **Figure 4D** and **Video S4**, the gripper started to open its fingers and then the P(OEGMA-DSDMA) layer was degraded gradually in this medium and showed similar biodegradation as compared to GSH. This experiment suggests that the soft grippers could be edible and biodegraded in the digestive tract as well or in the presence of administered Vitamin C.

CONCLUSION

In summary, we have demonstrated the first of their kind, multi-functional soft-robotic devices in the form of untethered microgrippers that are simultaneously thermomagnetically responsive, biocompatible and biodegradable. The gripers were fabricated using a photolithography approach which is highly parallel, cost-effective, and scalable. Various shapes for robotic or drug delivery structures can be created by varying the photomask design. Also, our materials recipe is compatible with alternate patterning approaches including 3D printing[44,45] and two photon crosslinking (TPC),[46,47] so that a range of other shapes could be fabricated.

The grippers respond to thermal stimuli allowing them to be opened or closed by heating such as with near infrared light, focused ultrasound or a hot patch. As previously demonstrated both in our work and the work of others, the LCST of gels can be tuned by synthetic approaches such as varying side chain length,[30] copolymerization with different monomers[48] and interpenetrating networks[49] in a wide range of temperatures compatible with actuation in the human body. The grippers are doped with magnetic nanoparticles allowing them to be manipulated from afar using clinical approaches; for example,

previously magnetic moieties have been guided using clinical MRI in animal models.[50,51] Another essential attribute is that the grippers are non-toxic and biodegradable either in naturally occurring disulfide reducing environments or on demand by administration of either GSH or Vitamin C. Our results also show that the UV exposure time and monomer concentration are important factors to consider and offer tunability in the time scale of biodegradation. We envision that this study moves the use of stimuli responsive biodegradable soft gripping robots closer to translation to the patient.

FIGURES

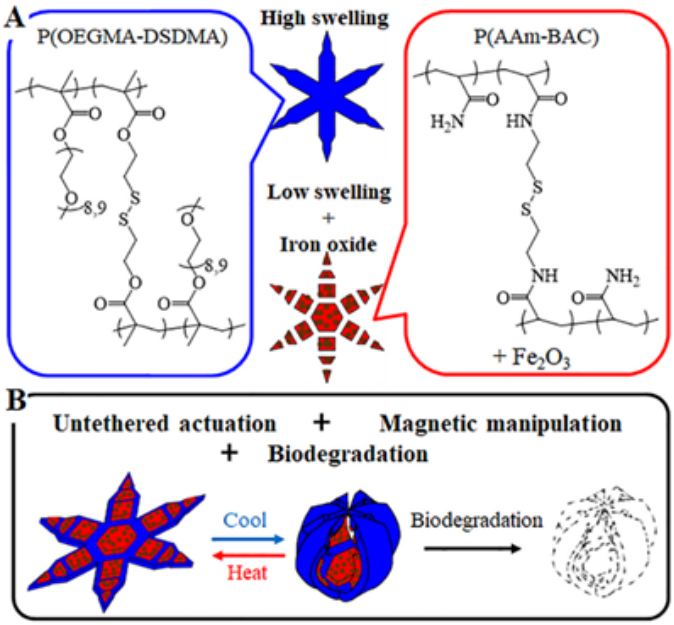

Figure 1. **Schematic of the molecular composition, structure, and operation of the biodegradable thermomagnetically responsive grippers. (A)** The grippers are composed of a bilayer of two hydrogels; a reversible high swelling P(OEGMA-DSDMA) gel and a low swelling P(AAm-BAC) gel. Also, magnetic Fe_2O_3 NPs are added within the P(AAm-BAC) gel. **(B)** Illustration of the multifunctional nature of the soft grippers including thermally responsive actuation, magnetic manipulation, and biodegradation.

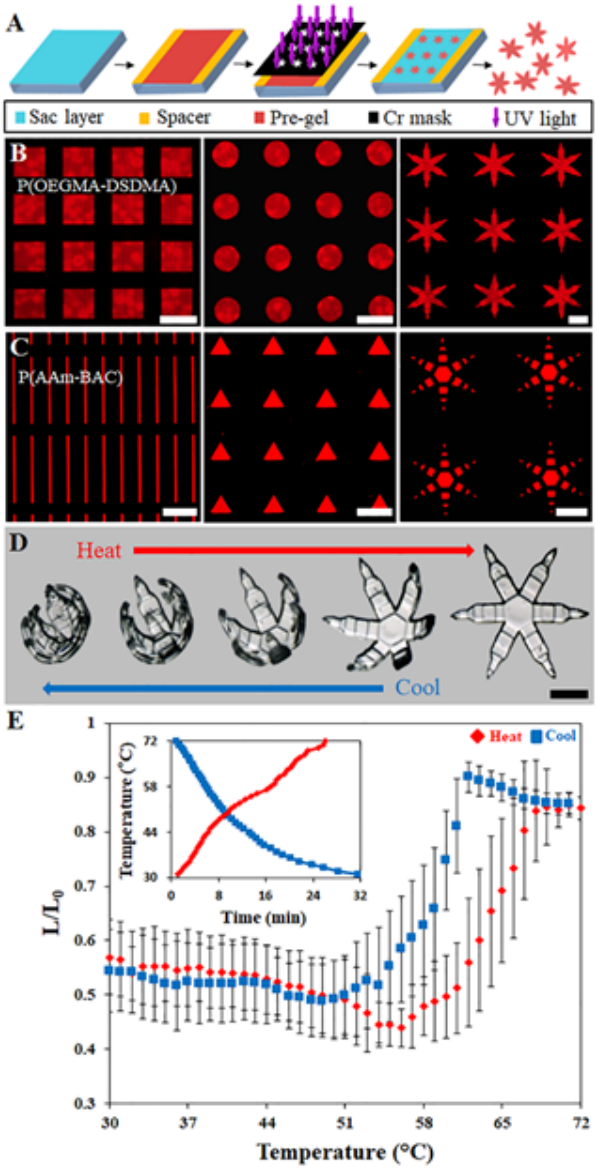

Figure 2. **Process flow for highly parallel photolithographic patterning of the P(OEGMA-DSDMA) and P(AAm-BAC) gels into specific shapes including thermally responsive grippers. (A)** Illustration of the photolithographic fabrication steps including deposition of a sacrificial alginate layer; assembly of a contact-mode chamber for photopatterning using spacers; exposure to UV light using CAD designed photomasks with registry; and release of the grippers from the substrate by dissolution of the sacrificial layer. **(B-C)** Fluorescence images of photopatterned and rhodamine stained, **(B)** P(OEGMA-DSDMA), and **(C)** P(AAm-BAC) gels with different shapes. The scale bar indicates a size of 2 mm. **(D)** Sequential optical images of photopatterned untethered P(OEGMA-DSDMA)/P(AAm-BAC) bilayer grippers that open on heating and close on cooling in a 1X PBS buffer solution. The scale bar indicates a size of 1.5 mm. **(E)** Graph of the normalized overall tip-to-tip length ratio (L/L_0) of the grippers at different steps during heating (red) and cooling (blue) in a 1X PBS buffer solution. A larger ratio indicates a more open gripper. The inset indicates the heating and cooling rate profile used during these measurements.

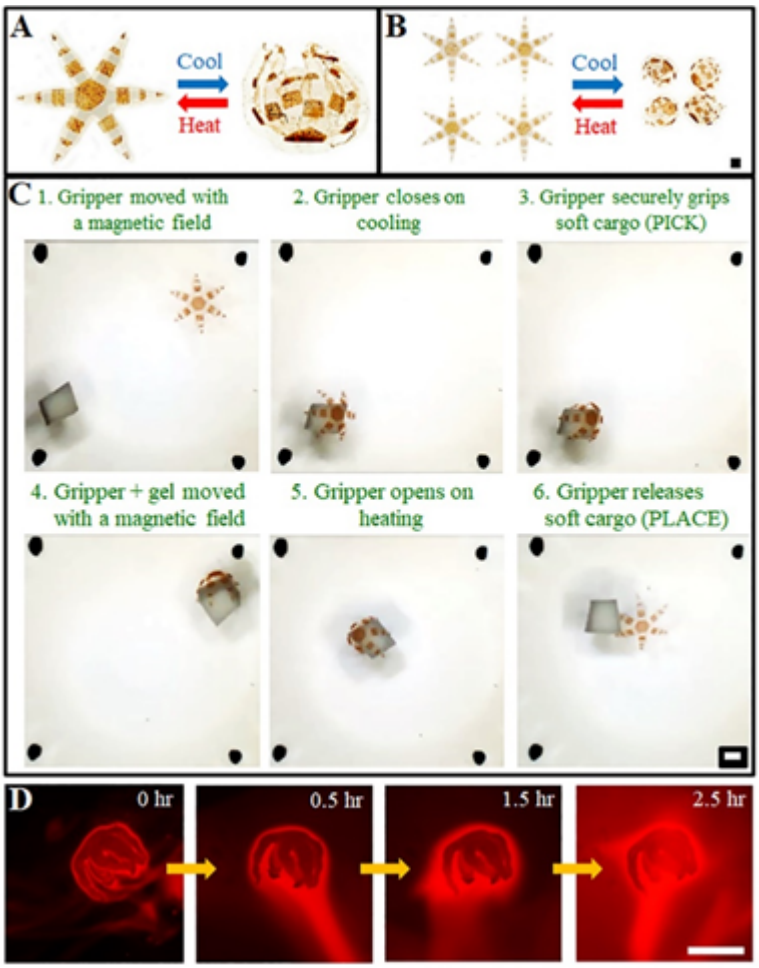

Figure 3. **Demonstration of thermomagnetically responsive operation and biodegradation of the soft grippers. (A)** Optical images of thermal actuation of the photopatterned soft grippers which are composed of a continuous transparent layer of a high swelling P(OEGMA-DSDMA) gel and brown segments of a Fe_2O_3 doped low swelling P(AAm-BAC) gel. The brown color in the segments is due to the Fe_2O_3 NPs. Either **(A)** single, or **(B)** many grippers close on cooling and open on heating. **(C)** Sequential optical images of magnetically guided and thermally actuated soft grippers to pick-and-place a soft cargo without any visible damages using a permanent magnet and a hot plate. **(D)** Optical fluorescence snapshots of the release of a rhodamine 6G dye at 25 ºC from dye loaded grippers indicating that they could be used for drug delivery. All scale bars indicate a size 2 mm.

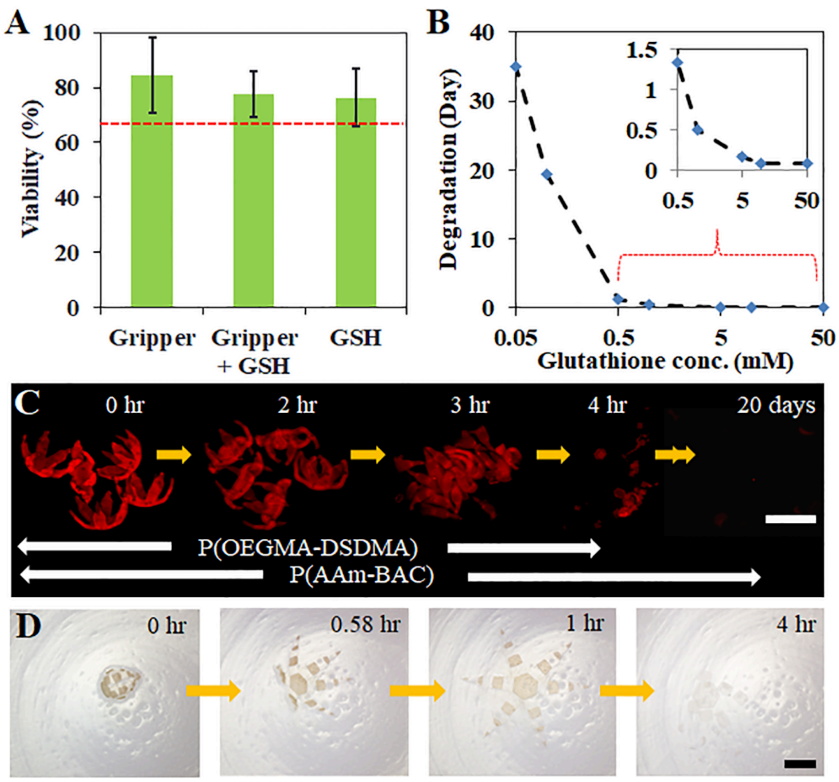

Figure 4. Biocompatibility and biodegradability of the soft grippers. **(A)** Results of the MTT assay test for three days contact with 1.95 x 10^5 cells/well of hTERT HAEC. The viability (% = OD_{570} / $OD_{570,\ control}$ x 100) which is greater than 70 % for all three samples indicates no cellular toxicity based on the ISO 10993-5 in-vitro assay for cytotoxicity of biomedical devices. We used the cell viability in the absence of both the gripper and GSH as the control sample to which all the data in the three bar graphs were normalized. **(B)** Biodegradability of a functional bilayer P(OEGMA-DSDMA) and P(AAm-BAC) gripper as a function of GSH concentration in the range of 50 microM to 50 mM; inset shows a magnified view of the graph in the range between 0.5 to 50 mM. Biodegradability was measured by noting the time at which the P(OEGMA-DSDMA) was no longer visible under an optical microscope, and the gripper broke into small pieces. The P(AAm-BAC) layer degrades more slowly and disappears after a longer time period. **(C)** Optical video snapshots of a functional bilayer P(OEGMA-DSDMA) and P(AAm-BAC) gripper at the high 50 mM GSH. Both layers that were dyed with a red fluorescent dye are no longer visible after 20 days. **(D)** Optical video snapshots of the biodegradation of a functional bilayer P(OEGMA-DSDMA) and P(AAm-BAC) gripper in 500 mM ascorbic acid (vitamin C) and 500 mM hydrogen peroxide at pH=3. All biodegradation experiments were done at physiological temperature of 37 ºC. Additional images during the degradation timeline are shown in Fig. S6.

ASSOCIATED CONTENT

Supporting Information. Details of the photolithographic chambers and Cr mask preparation. Details of the photopatternable, Fe_2O_3 containing AAm-BAC reaction solution. Process flow for photopatterning of the magnetic responsive soft grippers. Five supplementary figures and four supplementary videos are included. This material is available free of charge via the Internet at http://pubs.acs.org.

AUTHOR INFORMATION

Corresponding Author

*E-mail: dgracias@jhu.edu.

Author Contributions

D.H.G. conceived of the study. K.K, C.Y and S.H.O. performed experiments. J.V.P. performed MTT assay. The manuscript was written by D.H.G. K.K. and C.Y. and proofread by all the authors. #These authors contributed equally.

Notes

The authors declare no competing financial interest.

ACKNOWLEDGMENTS

We acknowledge financial support in part from the National Institutes of Health under Award RO1EB017742 and the National Science Foundation DMR-1709349. We also acknowledge funding from JSR Corporation and Kley Dom Biomimetics, LLC. The content is solely the responsibility of the authors and does not necessarily represent the official views of the funding agencies.

ABBREVIATIONS

P(OEGMA-DSDMA), poly[oligo ethylene glycol methyl ether methacrylate (M_n=500)-bis(2-methacryloyl)oxyethyl disulfide]; P(AAm-BAC), poly (acrylamide- *N*, *N*'- bis(acyloyl) cystamine); AAm, Acrylamide; OEGMA, Oligoethylene glycol methyl ether methacrylate (M_n=500); BAC, *N*,*N*'-

bis(acryloyl)cystamine; DSDMA, Bis(2-methacryloyl)oxyethyl disulfide; DMSO, dimethyl sulfoxide; Na-Alginate, sodium alginate; IPA, isopropyl alcohol; LCST, lower critical solution temperature; pNIPAM-AAc, poly (N-isopropylacrylamide-co-acrylic acid); PPF, polypropylene fumarate; DI H2O, deionized water; UV, ultraviolet; PBS, phosphate buffered saline; Fe_2O_3 NPs, iron oxide nanoparticles; GSH, glutathione.

References

(1) Fernandes, R.; Gracias, D. H. Toward a Miniaturized Mechanical Surgeon. *Mater. Today* **2009**, *12* (10), 14–20.

(2) Sitti, M.; Ceylan, H.; Hu, W.; Giltinan, J.; Turan, M.; Yim, S.; Diller, E. Biomedical Applications of Untethered Mobile Milli/Microrobots. *Proc. IEEE Inst. Electr. Electron. Eng.* **2015**, *103* (2), 205–224.

(3) Hu, C.; Pané, S.; Nelson, B. J. Soft Micro- and Nanorobotics. *Annual Review of Control, Robotics, and Autonomous Systems* **2018**, *1* (1), 53–75.

(4) Hu, Z.; Zhang, X.; Li, Y. Synthesis and Application of Modulated Polymer Gels. *Science* **1995**, *269* (5223), 525–527.

(5) Guan, J.; He, H.; Hansford, D. J.; James Lee, L. Self-Folding of Three-Dimensional Hydrogel Microstructures. *J. Phys. Chem. B* **2005**, *109* (49), 23134–23137.

(6) Bassik, N.; Abebe, B. T.; Laflin, K. E.; Gracias, D. H. Photolithographically Patterned Smart Hydrogel Based Bilayer Actuators. *Polymer* **2010**, *51* (26), 6093–6098.

(7) Stoychev, G.; Puretskiy, N.; Ionov, L. Self-Folding All-Polymer Thermoresponsive Microcapsules. *Soft Matter* **2011**, *7* (7), 3277-3279.

(8) Malachowski, K.; Breger, J.; Kwag, H. R.; Wang, M. O.; Fisher, J. P.; Selaru, F. M.; Gracias, D. H. Stimuli-Responsive Theragrippers for Chemomechanical Controlled Release. *Angew. Chem. Int. Ed.* **2014**, *53* (31), 8045-8049.

(9) Fusco, S.; Sakar, M. S.; Kennedy, S.; Peters, C.; Bottani, R.; Starsich, F.; Mao, A.; Sotiriou, G. A.; Pané, S.; Pratsinis, S. E.; Mooney, D.; Nelson, B. J. Targeted Delivery: An Integrated Microrobotic Platform for On-Demand, Targeted Therapeutic Interventions. *Adv. Mater.* **2014**, *26* (6), 952–957.

(10) Gracias, D. H. Stimuli Responsive Self-Folding Using Thin Polymer Films. *Curr. Opin. Chem. Eng.* **2013**, *2* (1), 112–119.

(11) Ionov, L. Hydrogel-Based Actuators: Possibilities and Limitations. *Mater. Today* **2014**, *17* (10), 494–503.

(12) Cangialosi, A.; Yoon, C.; Liu, J.; Huang, Q.; Guo, J.; Nguyen, T. D.; Gracias, D. H.; Schulman, R. DNA Sequence-Directed Shape Change of Photopatterned Hydrogels via High-Degree Swelling. *Science* **2017**, *357* (6356), 1126–1130.

(13) Breger, J. C.; Yoon, C.; Xiao, R.; Kwag, H. R.; Wang, M. O.; Fisher, J. P.; Nguyen, T. D.; Gracias, D. H. Self-Folding Thermo-Magnetically Responsive Soft Microgrippers. *ACS Appl. Mater. Interfaces* **2015**, *7* (5), 3398–3405.
(14) Ghosh, A.; Yoon, C.; Ongaro, F.; Scheggi, S.; Selaru, F. M.; Misra, S.; Gracias, D. H. Stimuli-Responsive Soft Untethered Grippers for Drug Delivery and Robotic Surgery. *Front. Mech. Eng.* **2017**, *3*, 7.
(15) Gultepe, E.; Yamanaka, S.; Laflin, K. E.; Kadam, S.; Shim, Y.; Olaru, A. V.; Limketkai, B.; Khashab, M. A.; Kalloo, A. N.; Gracias, D. H.; Selaru, F. M. Biologic Tissue Sampling with Untethered Microgrippers. *Gastroenterology* **2013**, *144* (4), 691–693.
(16) Nemeth, A.; Wurm Johansson, G.; Nielsen, J.; Thorlacius, H.; Toth, E. Capsule Retention Related to Small Bowel Capsule Endoscopy: A Large European Single-Center 10-Year Clinical Experience. *United European Gastroenterol J* **2017**, *5* (5), 677–686.
(17) Tibbitt, M. W.; Dahlman, J. E.; Langer, R. Emerging Frontiers in Drug Delivery. *J. Am. Chem. Soc.* **2016**, *138* (3), 704–717.
(18) Li, J.; Mooney, D. J. Designing Hydrogels for Controlled Drug Delivery. *Nat Rev Mater* **2016**, *1* (12), 16071.
(19) Park, H.; Park, K.; Shalaby, W. S. W. *Biodegradable Hydrogels for Drug Delivery*; CRC Press, **1993**.
(20) Gan, J.; Guan, X.; Zheng, J.; Guo, H.; Wu, K.; Liang, L.; Lu, M. Biodegradable, Thermoresponsive PNIPAM-Based Hydrogel Scaffolds for the Sustained Release of Levofloxacin. *RSC Adv.* **2016**, *6* (39), 32967–32978.
(21) Lee, M. H.; Yang, Z.; Lim, C. W.; Lee, Y. H.; Dongbang, S.; Kang, C.; Kim, J. S. Disulfide-Cleavage-Triggered Chemosensors and Their Biological Applications. *Chem. Rev.* **2013**, *113* (7), 5071–5109.
(22) Fass, D.; Thorpe, C. Chemistry and Enzymology of Disulfide Cross-Linking in Proteins. *Chem. Rev.* **2018**, *118* (3), 1169–1198.
(23) Lutz, J. -F. Polymerization of Oligo(Ethylene Glycol) (Meth)AcrylatesToward New Generations of Smart Biocompatible Materials, 2008, Journal of Polymer Sci. Part A.pdf. *Journal of Polymer Science: Part A: Polymer Chemistry*. **2008**, 3459–3470.
(24) Roth, P. J.; Jochum, F. D.; Forst, F. R.; Zentel, R.; Theato, P. Influence of End Groups on the Stimulus-Responsive Behavior of Poly[Oligo(Ethylene Glycol) Methacrylate] in Water. *Macromolecules* **2010**, *43* (10), 4638–4645.
(25) Dong, H.; Matyjaszewski, K. Thermally Responsive P(M(EO)2MA-co-OEOMA) copolymers via AGET ATPR in miniemulsion. *Macromolecules* **2010,** *43* (10), 4623-4628.
(26) Kotsuchibashi, Y.; Narain, R. Dual-Temperature and pH Responsive (Ethylene Glycol)-Based Nanogels via Structural Design. *Polym. Chem.* **2014**, *5* (8), 3061–3070.
(27) King, D. J.; Noss, R. R. Toxicity of Polyacrylamide and Acrylamide Monomer. *Rev. Environ. Health* **1989**, *8* (1-4), 3–16.
(28) Kandow, C. E.; Georges, P. C.; Janmey, P. A.; Beningo, K. A. Polyacrylamide Hydrogels for Cell Mechanics: Steps toward Optimization and Alternative Uses. *Methods Cell Biol.* **2007**, *83*, 29–46.
(29) Jamal, M.; Kadam, S. S.; Xiao, R.; Jivan, F.; Onn, T.-M.; Fernandes, R.; Nguyen, T. D.; Gracias, D. H. Bio-Origami Hydrogel Scaffolds Composed of Photocrosslinked PEG Bilayers. *Adv. Healthc. Mater.* **2013**, *2* (8), 1142–1150.

(30) Kobayashi, K.; Oh, S. H.; Yoon, C.; Gracias, D. H. Multitemperature Responsive Self-Folding Soft Biomimetic Structures. *Macromol. Rapid Commun.* **2018**, *39* (4), 1700692.
(31) Garstecki, P.; Tierno, P.; Weibel, D. B.; Sagués, F.; Whitesides, G. M. Propulsion of Flexible Polymer Structures in a Rotating Magnetic Field. *J. Phys. Condens. Matter* **2009**, *21* (20), 204110.
(32) Yamanishi, Y.; Sakuma, S.; Onda, K.; Arai, F. Biocompatible Polymeric Magnetically Driven Microtool for Particle Sorting. *Journal of Micro-Nano Mechatronics* **2008**, *4* (1-2), 49–57.
(33) Sakar, M. S.; Steager, E. B.; Kim, D. H.; Kim, M. J.; Pappas, G. J.; Kumar, V. Single Cell Manipulation Using Ferromagnetic Composite Microtransporters. *Appl. Phys. Lett.* **2010**, *96* (4), 043705.
(34) Ongaro, F.; Scheggi, S.; Yoon, C.; den Brink, F. van; Oh, S. H.; Gracias, D. H.; Misra, S. Autonomous Planning and Control of Soft Untethered Grippers in Unstructured Environments. *J Microbio Robot* **2017**, *12* (1-4), 45–52.
(35) Kim, Y.; Yuk, H.; Zhao, R.; Chester, S. A.; Zhao, X. Printing Ferromagnetic Domains for Untethered Fast-Transforming Soft Materials. *Nature* **2018**, *558* (7709), 274–279.
(36) Khatib, K. A.; Aramouni, F. M.; Herald, T. J.; Boyer, J. E. Physicochemical Characteristics of Soft Tofu Formulated from Selected Soybean Varieties. *J. Food Qual.* **2002**, *25* (4), 289–303.
(37) Butcher, D. T.; Alliston, T.; Weaver, V. M. A Tense Situation: Forcing Tumour Progression. *Nat. Rev. Cancer* **2009**, *9* (2), 108–122.
(38) He, H.; Guan, J.; Lee, J. L. An Oral Delivery Device Based on Self-Folding Hydrogels. *J. Control. Release* **2006**, *110* (2), 339–346.
(39) Black, J. *Biological Performance of Materials: Fundamentals of Biocompatibility, Fourth Edition*; CRC Press, **2005**.
(40) International Organization for Standardization. Biological evaluation of medical devices – ISO 10993, Part 5: Tests for in vitro cytotoxicity. Geneva, Switzerland; **1999**.
(41) Meister, A.; Anderson, M. E. Glutathione. *Annu. Rev. Biochem.* **1983**, *52*, 711–760.
(42) Xu, C.; Huang, Y.; Wu, J.; Tang, L.; Hong, Y. Triggerable Degradation of Polyurethanes for Tissue Engineering Applications. *ACS Appl. Mater. Interfaces* **2015**, *7* (36), 20377–20388.
(43) Ruiz, J. J.; Aldaz, A.; Dominguez, M. Mechanism of L-Ascorbic Acid Oxidation and Dehydro-L-Ascorbic Acid Reduction on a Mercury Electrode. I. Acid Medium. *Can. J. Chem.* **1977**, *55* (15), 2799-2806.
(44) Mannoor, M. S.; Jiang, Z.; James, T.; Kong, Y. L.; Malatesta, K. A.; Soboyejo, W. O.; Verma, N.; Gracias, D. H.; McAlpine, M. C. 3D Printed Bionic Ears. *Nano Lett.* **2013**, *13* (6), 2634–2639.
(45) Gladman, A. S.; Matsumoto, E. A.; Nuzzo, R. G.; Mahadevan, L.; Lewis, J. A. Biomimetic 4D Printing. *Nat. Mater.* **2016**, *15* (4), 413–418.
(46) Kim, S.; Qiu, F.; Kim, S.; Ghanbari, A.; Moon, C.; Zhang, L.; Nelson, B. J.; Choi, H. Fabrication and Characterization of Magnetic Microrobots for Three-Dimensional Cell Culture and Targeted Transportation. *Adv. Mater.* **2013**, *25* (41), 5863–5868.
(47) Ceylan, H.; Yasa, I. C.; Sitti, M. 3D Chemical Patterning of Micromaterials for Encoded Functionality. *Adv. Mater.* **2017**, *29* (9), 1605072.
(48) So, S.; Hayward, R. C. Tunable Upper Critical Solution Temperature of Poly(N-Isopropylacrylamide) in Ionic Liquids for Sequential and Reversible Self-Folding. *ACS Appl. Mater. Interfaces* **2017**, *9* (18), 15785–15790.

(49) Zheng, W. J.; An, N.; Yang, J. H.; Zhou, J.; Chen, Y. M. Tough Al-alginate/Poly(N-Isopropylacrylamide) Hydrogel with Tunable LCST for Soft Robotics. *ACS Appl. Mater. Interfaces* **2015**, *7* (3), 1758–1764.
(50) Martel, S.; Mathieu, J.-B.; Felfoul, O.; Chanu, A.; Aboussouan, E.; Tamaz, S.; Pouponneau, P.; Yahia, L.; Beaudoin, G.; Soulez, G.; Mankiewicz, M. Automatic Navigation of an Untethered Device in the Artery of a Living Animal Using a Conventional Clinical Magnetic Resonance Imaging System. *Appl. Phys. Lett.* **2007**, *90* (11), 114105.
(51) Martel, S. Beyond Imaging: Macro- and Microscale Medical Robots Actuated by Clinical MRI Scanners. *Science Robotics* **2017**, *2* (3), eaam8119.

TOC graphic

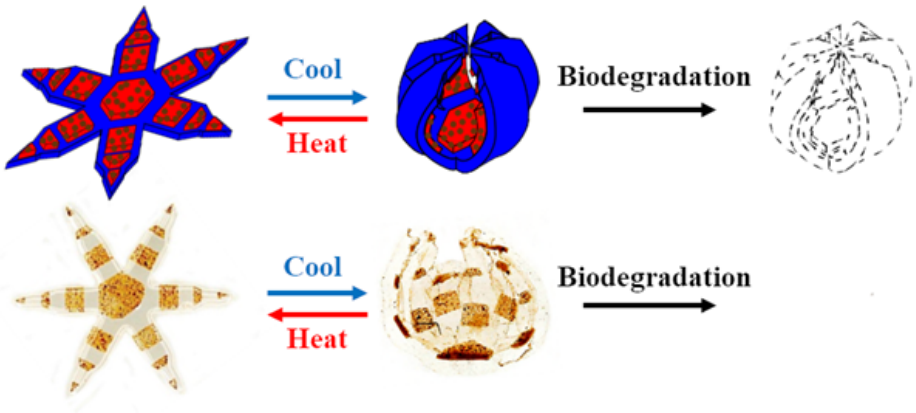

Supporting Information

Biodegradable thermomagnetically responsive soft untethered grippers

Kunihiko Kobayashi[#†§], ChangKyu Yoon[#‡†], Seung Hyun Oh[†], Jayson V. Pagaduan[†] & David H. Gracias[*‡†]

[†] Department of Chemical and Biomolecular Engineering, The Johns Hopkins University, Baltimore, MD 21218, USA.

[‡] Department of Materials Science and Engineering, The Johns Hopkins University, Baltimore, MD 21218, USA.

[†] Present address: Department of Mechanical Systems Engineering, Sookmyung Women's University, Seoul, Republic of Korea.

[§] JSR Corporation, 1-9-2, Higashi-Shimbashi, Minato-ku, Tokyo 105-8640, Japan.

[#] K. Kobayashi and Dr. C. Yoon contributed equally to this work.

* Corresponding Author: email: dgracias@jhu.edu

KEYWORDS: *stimuli responsive materials, hydrogels, soft robotics, bioMEMS, actuators*

S1. Details of the fabrication process

S1. 1. Fabrication of chromium photomasks

We observed significantly higher resolution and lower adhesion of gels to chromium masks. We first designed photomasks using AutoCAD and the masks were printed on a Mylar film (Fineline, Imaging). These transparency masks were used to fabricate chromium (Cr) masks on glass using established processes. Briefly, glass slides (2 inches by 2 inches, VWR) were rinsed with acetone, methanol, and isopropyl alcohol, and then dried with a stream of nitrogen gas. SC 1827 photoresist was spin coated on the clean glass surface at 3000 rpm and baked at 115°C for 1 min. Then, the glass slides were exposed to UV light through the photomasks at ~160 mJ/cm^2 and developed in 351 Developer (Rohm and Haas) in deionized (DI) water (1:5 volume ratio) for 50 s. The patterned glass slides were cleaned using an oxygen plasma (Plasma Etch) for 2 min at a radio frequency (RF) power of 100 W and oxygen flow of 20 sccm. Then, 200 nm of Cr was deposited onto the plasma-cleaned glass slides by thermal evaporation, and finally the glass slides were immersed in an acetone bath to dissolve the photoresist. The Cr masks were coated by Cytop at a speed 3000 rpm and baked at 70 °C for overnight before use. The tip-to-tip size of the grippers on the Cr mask was 4 mm.

Contact-mode chambers for photolithography

Contact-mode chambers were used to pattern the gels using photolithography. The top side of the chambers was a chromium (Cr) photomask. The bottom side of the contact mode chambers were prepared by spin coating a sodium alginate solution (Na-alginate (Sigma-Aldrich) : DI H2O = 2: 100 (w/w)) at 2000 rpm for 1 minute on top of a glass slide and then dried at 115 °C for 5 minutes. The spin coated Na-alginate layer served as a sacrificial layer which was dissolved in 1x PBS buffer solution to lift off (release) the photopatterned gels from the glass slide.

Preparation of the photopatternable Fe_2O_3 doped AAm-BAC pre-gel solution

An AAm-BAC stock solution was prepared by dissolving AAm and BAC in DMSO at 20 wt % of the total monomer concentration. The BAC/(BAC+AAm) concentration was 20 %. A stock solution of Fe_2O_3 and AAm-BAC was prepared by adding Fe_2O_3 NPs in an AAm-BAC stock solution. The concentration of Fe_2O_3 NPs /(BAC+AAm) was adjusted to 5.3 %. The Fe_2O_3 doped AAm-BAC pre-gel solution was prepared by mixing the stock solution and Irgacure 2100 at a volume ratio of 100:1, just before use.

Photopatterning of the magnetically responsive soft grippers

150 µl of the AAm-BAC reaction solution with Fe_2O_3 was deposited on the Na-Alginate coated glass slide and contacted with a Cr mask. Spacers approximately 32 µm thick were used between the Cr mask and the Na-alginate coated glass slide. Gels were photopatterned using a UV lamp where the irradiation intensity was adjusted to 81 mJ/cm^2. After photopatterning, the glass slide was washed with IPA and then dried with a stream of nitrogen gas. 300 µl of OEGMA- DSDMA reaction solution was deposited on the patterned glass slide and contact with a Cr mask. Spacers approximately 64 µm thick were used between the Cr mask and the glass slide. Gels were photopatterned using a UV lamp and the UV irradiation intensity was adjusted at 81 mJ/cm^2. After photopatterning, the glass slide was washed with IPA and then dried with a stream of nitrogen gas. The grippers were lifted-off in 1x PBS solution.

Supplementary Figures

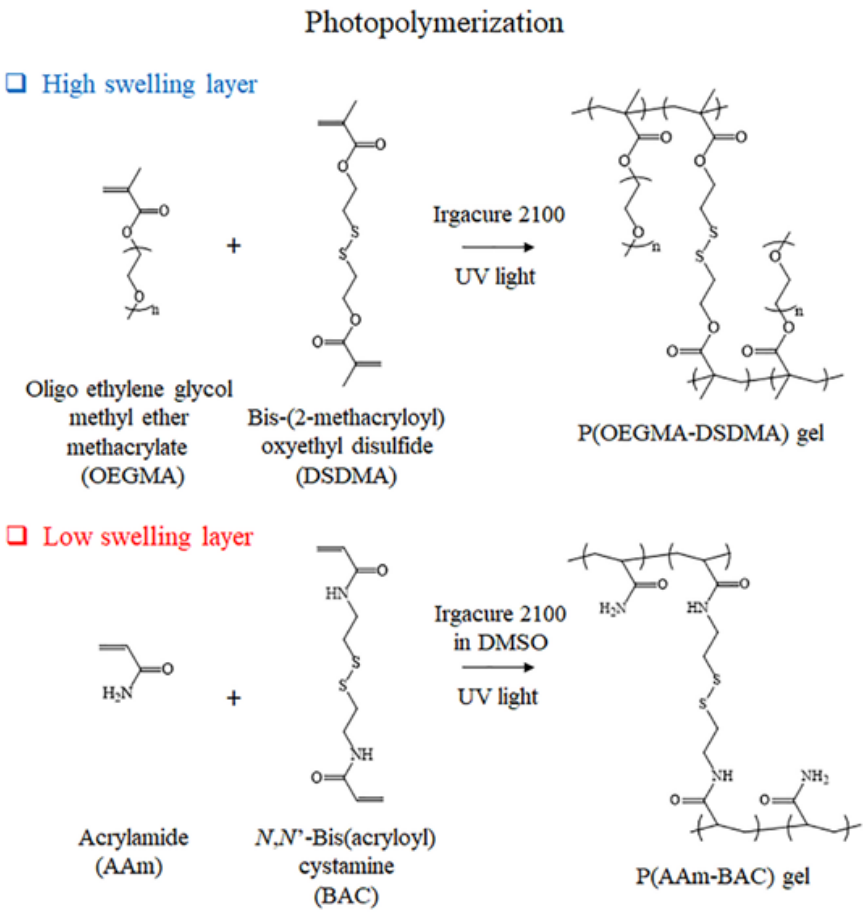

Figure S1. Schematic illustration of the molecular composition and UV photopatterning of high swelling P(OEGMA-DSDMA) and low swelling P(AAm-BAC) gels in a bilayer.

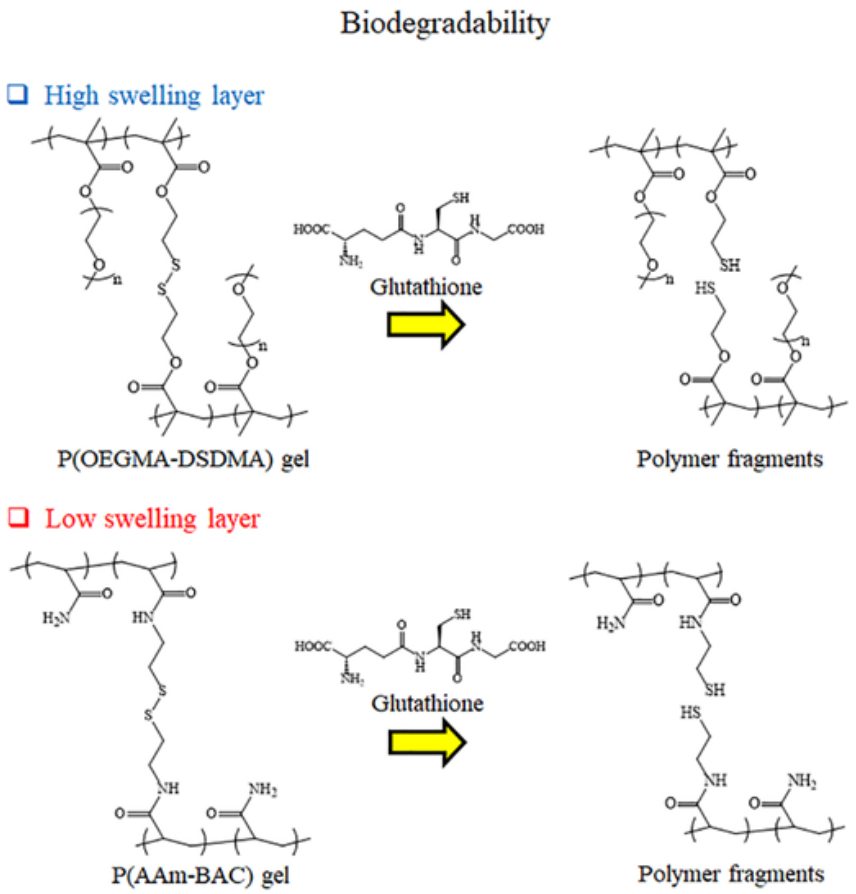

Figure S2. Schematic illustration of the biodegradability mechanism of the P(OEGMA-DSDMA) P(AAm-BAC) gels by reducing agents such as glutathione (GSH).

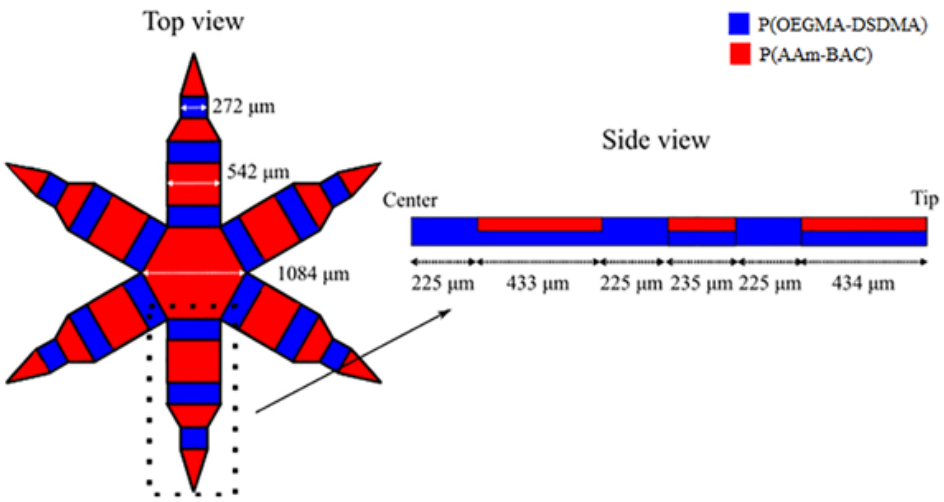

Figure S3. Top and side view dimensions of the multi-fingered gripper with a continuous layer of the high swelling P(OEGMA-DSDMA) gel, shown in blue, and segments of the low swelling P(AAm-BAC) gel shown in red.

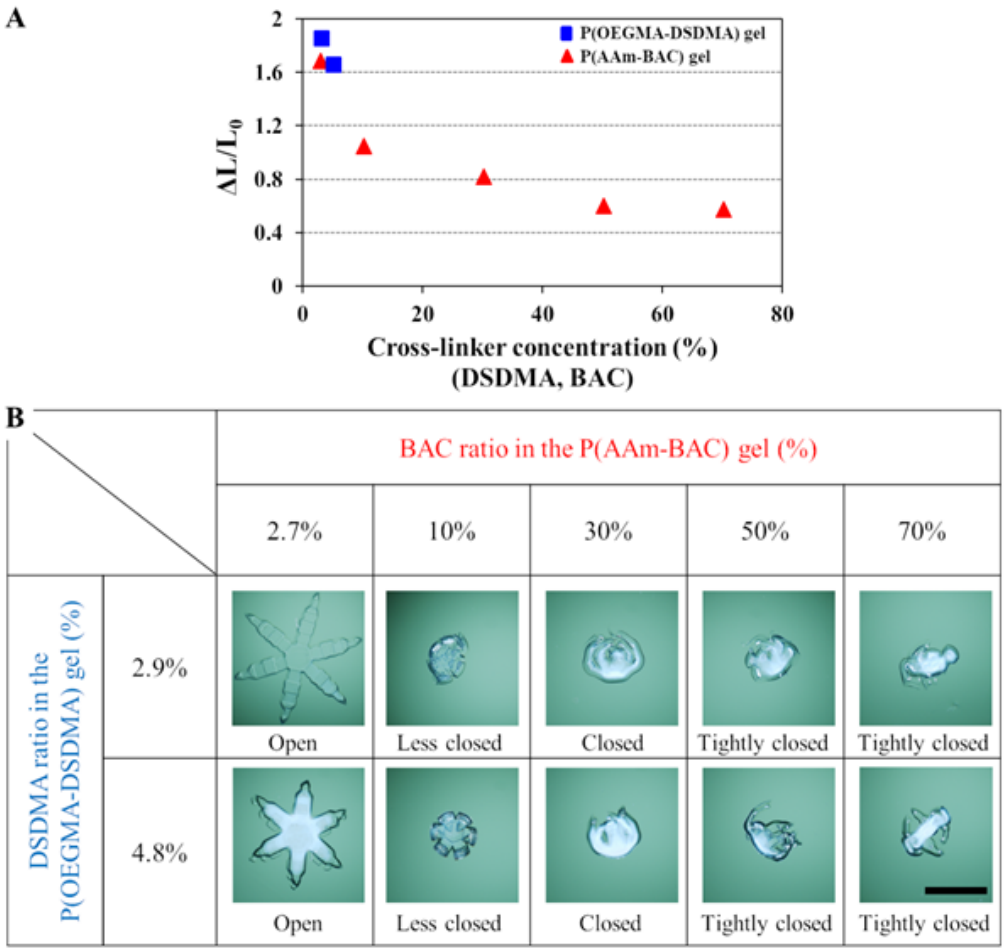

Figure S4. (A) Linear swelling ratio defined as a percentage of the increase in length divided by the original photopatterned length of P(OEGMA-DSDMA) and P(AAm-BAC) gel squares on immersion in PBS at room temperature for different concentrations of DSDMA (blue) and BAC (red). (B) Images of grippers after immersion in PBS at room temperature as a function of DSDMA ratio of 2.9 and 4.8 % and BAC ratio of 2.7 to 70%. The results indicate that low concentrations of both DSDMA and BAC result in flat non-functional grippers, but a low concentration of DSDMA (high swelling gel) and a high concentration of BAC (low swelling gel) results in optimal grippers.

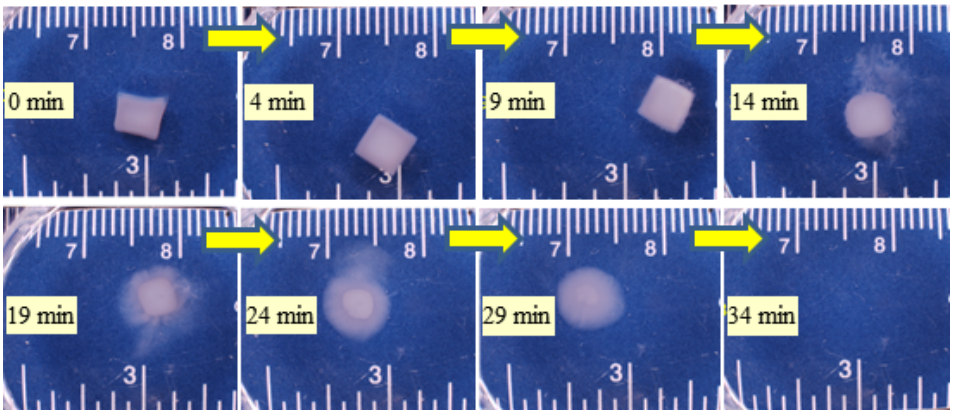

Figure S5. Representative video snapshots of the biodegradation of a cube-shaped P(AAm-BAC) hydrogel synthesized with 2.7% BAC concentration in 50 mM glutathione in phosphate buffer at 37 °C. A higher BAC ratio requires longer time for biodegradation while a lower BAC ratio required a shorter biodegradation time.

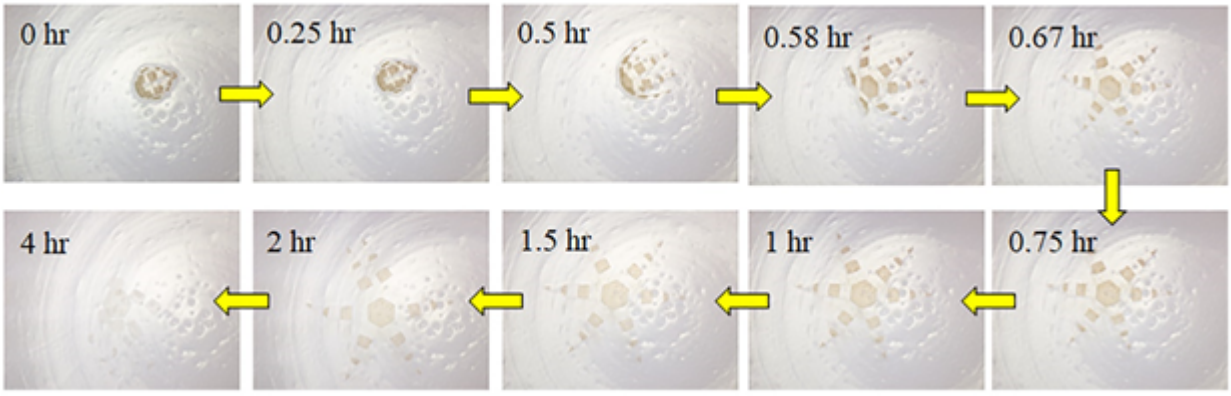

Figure S6. More detailed representative snapshots of the biodegradation of P(OEGMA-DSDMA) based soft grippers as shown in Figure 4D. The Vitamin C driven biodegradation test was done for four hours with 500 mM ascorbic acid and 500 mM hydrogen peroxide, pH=3 at 37 °C.

Table S1. Biodegradability measurements of P(OEGMA-DSDMA) cube gels over 24 hours with varying monomer concentration and UV exposure time at 37 °C in a GSH solution.

Hydrogel (#)	Monomer concentration (wt %)	UV exposure (second)	Biodegradation at 37 °C
1	100	150	Yes
2	100	300	No
3	100	450	No
4	80	188	Yes
5	80	376	No
6	80	564	No
7	60	500	Yes
8	60	750	Yes
9	60	1000	Yes

Yes: Fully degraded
No: NOT Fully degraded

Supplementary video S1. Video microscopy clip (x64) showing the opening of the soft grippers on heating from 37 °C to 72 °C and closing of the soft grippers and on cooling from 72 °C to 37 °C. The average heating ramp was 1 °C/min.

Supplementary video S2. Video microscopy clip showing a representative pick-and-place test using the thermomagnetically responsive soft grippers. The grippers opened their fingers approximately at 70 °C and then could be magnetically guided them using a permanent magnetic bar to a soft cargo, soft tofu (x3). Then, the soft grippers closed their fingers to pick the tofu when heat was cool down by 37 °C (x64). The soft grippers then grabbed the tofu and could be guided again to another target area using a permanent magnetic bar (x3). Finally, the soft grippers released the cargo at the second target site when heated up.

Supplementary video S3. Video microscopy clip showing dye diffusion from rhodamine 6G loaded, biodegradable soft grippers at 25°C.

Supplementary video S4. Video microscopy clip showing biodegradation of a thermomagnetically responsive soft gripper in GSH solution.